

# Monte-Carlo modeling of optical sensors for postoperative free flap monitoring \*

Paulina Stadnik<sup>1</sup>, Ignacy Rogoń<sup>1</sup><sup>[0000-0002-6630-7086]</sup>, and Mariusz Kaczmarek<sup>1</sup><sup>[000-0001-6488-7489]</sup>

Biomedical Engineering Department, Gdańsk University of Technology, Narutowicza 11/12 Str., 80-233 Gdańsk, Poland  
{ignacy.rogon, markaczm}@pg.edu.pl

**Abstract.** This work aims to develop a numerical tissue model and implement software to simulate photon propagation using the Monte Carlo method to determine design guidelines for a physical measurement system. C++ was used for the simulation program, and Python as a programming environment to create an interface that allows the user to customize individual simulation elements, allowing for increased accuracy and flexibility when simulating photon movement. This allows the user to customize the simulation to their specific requirements, ensuring the results are as accurate and reliable as possible. It also models the detector to determine if a given photon is in the desired location. The program simulates the propagation of light from a normal illumination medium with anisotropic scattering and records the escape of photons on the upper surface. The simulation also takes into account absorption and scattering coefficients for a given wavelength, and data regarding these parameters are read from a .csv file. The variance reduction technique is used to improve the efficiency of the simulation. The user interface allows users to define their own parameters, such as wavelength, anisotropy coefficient, refractive index, and layer thickness. In this paper, we simulate four photodiodes and different distances between the source and detector to determine the most suitable model for designing a physical sensor.

**Keywords:** Monte-Carlo simulation · Light sensor · Photodiode · Optics · Photon · Light propagation · Skin tissue.

## 1 Introduction

The International Agency for Research on Cancer reported that in 2020 breast cancer became the world's most commonly diagnosed cancer type. Over 2.26 million new cases of breast cancer and almost 685 000 deaths were reported. Breast cancer was the most common cause of cancer death in women and the fifth most common cause of cancer death overall [1]. Moreover, every year, 1.7 million people in Europe are diagnosed with cancer, almost half of whom die.

---

\* Supported by Statutory Funds of Electronics, Telecommunications and Informatics Faculty, Gdansk University of Technology.

Analyzing the above statistics, it can be seen that cancer is a huge problem not only in terms of health but also socially. It is estimated that in 2000 in European Union, around 25,000 women were diagnosed with breast cancer, which is about 25% of all cancers diagnosed in women [2]. In 2009 analysis [3] prepared by researchers at Maria Skłodowska-Curie Polish National Oncology Centre, incidence and mortality predictions for cancer in Poland up to the year 2025 were presented. The prognosis for the years 2010-2025 indicated an increasing trend of breast cancer incidence for all age groups. The forecast stated that in 2025, the number of new breast cancer cases is expected to be almost 50% higher than the one observed in 2006. The highest increase of new cancer cases is expected for women aged 50 years and more, with over half of the cases occurring between the 50th and 69th year of life. The researchers stated that the number of deaths due to breast cancer would increase, while the proportion of deaths for each age group would change. In 2006 about half of the deaths fell on women before the age of 70, 2025 one should expect a decrease in the number of deaths in this age group to about 30%, while almost 70% of deaths due to breast cancer would occur for the oldest women (after the age of 70). A mastectomy, supported by other therapies, is one of the basic methods of treating breast cancer. The consequence of mastectomy is a further treatment involving the reconstruction of the removed breast. This is done by various methods: implantation of silicone implants or by transplantation of own tissues. Tissue transplantation is used in surgical defect reconstructions when suturing existing tissues impossible. It is also used in the area of breast cancer diseases and is used to reconstruct the shape of the breast after the tumor is removed. One of the side effects of reconstructive surgery may be tissue ischemia. This means there is not enough blood flow, which can lead to tissue damage or even death. This phenomenon can have serious consequences for patients after breast cancer surgery, including an increased risk of postoperative complications and longer wound healing time. To prevent this, blood-supplying vessels should be monitored for a period of up to 72 hours after the procedure. One of the most promising techniques in analyzing tissue blood flow is light-based methods [4]. The behavior of light in tissues is an important topic in many fields, including medicine, where it can be used to diagnose diseases and monitor treatment processes. Light can behave in two main ways in tissues: scattering and absorption. The scattering coefficient measures the ability of particles to scatter photons, while the absorption coefficient measures the amount of photons absorbed at a given distance. These parameters are important in determining how light travels through tissues. Both mentioned processes are random, making the Monte Carlo method ideal for simulating them. In this paper, a Monte Carlo method in simulations of photons behavior in modeled tissue is presented. A few existing sensors (photodiodes) were simulated to determine the most suitable for future system design.

## 2 Theoretical basis

Most tissues in the human body are carriers with a high degree of scattering and variable absorbance both in the visible and non-visible range. In most cases, photons are scattered multiple times before being absorbed. Simulating the paths of photons is too complex to be modeled analytically. Often, instead of a manual and tedious process, Monte Carlo simulations are used to streamline this work [5][6].

### 2.1 Skin Tissue model

An anatomical tissue model is a virtual or physical representation of the tissue structure of the human or animal body, which is particularly useful in many fields, such as medicine, biology, and materials science. The model is made up of different layers that contain various elements, such as epithelial cells, connective tissue cells, collagen, and elastin, as well as information about the physical, chemical, and biological properties of the tissues. The skin consists of a layered epithelium containing differentiated keratinocytes (cells responsible for the production of keratin in the skin) that are cultured on a shrunken collagen matrix filled with dermal fibroblasts (connective tissue cells found in the dermis responsible for the production of collagen and elastin, the most important supporting proteins of the skin, determine its strength, density, flexibility, and elasticity) [7]. We assume that our model is nonuniform and consists of three layers - see Fig. 1a:

- skin - understood as two layers together: the epidermis and dermis, width = 3.5mm,
- fat - laying unfed the skin layer, width 10mm,
- muscle - deepest layer, width = 11.2mm.

It should be emphasized that we model the structure of the skin and subcutaneous tissues for the thoracic region and the breast itself.

**Tissue modeling** One of the most important properties of tissues is their ability to absorb, scatter, or reflect light, which is important in many diagnostic and therapeutic techniques, such as laser treatment of eye diseases or photodynamic therapy of cancer, and in imaging by various technologies, such as computed tomography or magnetic resonance imaging. The tissue model can also be used in skin research to model and explain physical phenomena such as light absorption, reflection, and light scattering and to study the influence of external factors such as ultraviolet radiation, temperature, and humidity on skin properties. The Monte Carlo (MC) method is based on the random walk technique and is used to simulate the behavior of light in tissue. It is a valuable tool for medicine in diseases such as cancer. It is also useful for studying the effect of anisotropy on the propagation of light in the tissue and for determining the spatial distribution of optical parameters in the tissue.

There are methods for accurately mapping human organs. Modeled human tissues can be used in various stages of diseases if they faithfully reflect the shape,

size, or, above all, the properties of the desired organ. Biomechanical modeling opens many areas of medical activity to new possibilities. Implementation of tissue modeling methods, however, often requires linear connections, and models do not always lead to satisfactory results. Non-linear models were introduced to overcome the limitations of linear solutions. The development of this method is facilitated by special frameworks dedicated to the creation of algorithms and simulators. Such tools allow researchers to focus on the essence of the problem [8].

Mathematical models of tissues make it possible to identify biological processes occurring in the human body and form the basis for simulations. Many methods of tissue modeling were found in the articles cited in the paper. In the available literature, methods such as the elastic-mass method and the finite element method were found. The former allows for complex real-time simulations. It describes the mechanical properties of tissue through a grid of points connected by weightless, flexible springs and optional shock absorbers. Each point has specific parameters, such as weight and position, and its trajectory is set according to Newton's law of motion. This method is used in surgical simulation. It is easy to implement and does not require a lot of computing power.

## 2.2 Light behavior in tissue

Scattering of light occurs to some degree in all media except vacuum and depends on the heterogeneity of the medium down to the atomic level. Charges in the matter are set in motion by passing electromagnetic waves. Moving charges emit secondary radiation in all directions, producing diffuse waves. The final radiation distribution is the sum of the incident and scattered waves.

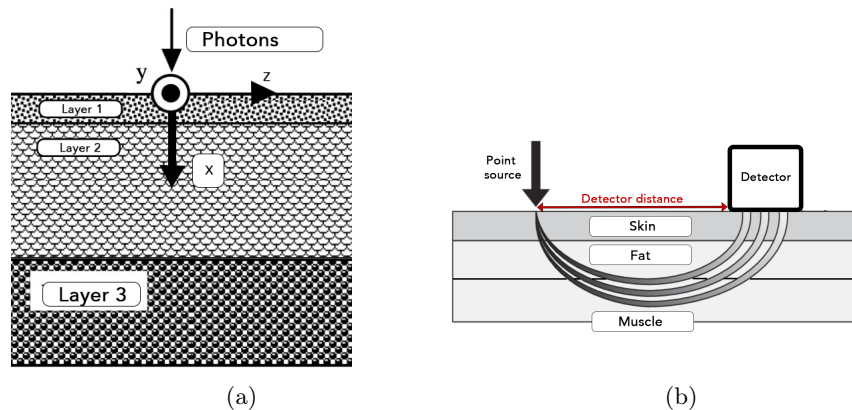


Fig. 1: (a) - Numerical model of the skin tissue used in simulations. The y-axis points outward [10]; (b)- Principle idea behind tracking the behavior of photons in the tissue. Please note that detector distance is measured to its closest edge

The scattering coefficient is a measure of the particle's ability to scatter photons from a beam of light, while the absorption coefficient is a measure of how many photons have been absorbed. Each parameter is expressed as a number proportional to the number of photons scattered or absorbed over a distance.

If a beam of optical radiation propagates through a medium in which there is more than one scattering center, then optical radiation can be scattered not only singly but also many times. The scattering properties of such a medium depend not only on the properties of individual mediums but also on the spatial density of their occurrence and spatial order. Knowing the cross-sections of the scattering centers  $\sigma_s$  and their spatial density  $\rho_s$ , the scattering coefficient for this medium can be determined (1):

$$\mu_s = \sigma_s \cdot \rho_s \quad (1)$$

An alternative to light scattering is its conversion into heat, i.e., absorption. From the law of conservation of energy, when absorbing a photon, its energy depends on the frequency of the light (2):

$$\Delta E = h\nu = \frac{hc}{\lambda} = \frac{2\pi hc}{k}, \quad (2)$$

where:  $h$  - Planck constant,  $c$  - speed of light in a vacuum,  $\lambda$  - length of the absorbed wavelength,  $\nu$  - vibration frequency,  $k$  - wave number.

To simplify notation, the total interaction coefficient  $\mu_t$  is sometimes used, which is the sum of the absorption coefficient  $\mu_a$  and the dispersion coefficient  $\mu_s$ . Consequently, the interaction coefficient denotes the probability of photon interaction per unit of infinitesimal path length.

By analogy to formula (1), the absorption coefficient for this medium can be determined (3):

$$\mu_a = \sigma_a \cdot \rho_a, \quad (3)$$

where  $\sigma_a$  are the cross-sections of the scattering centers, and their spatial density is  $\rho_a$ .

The extinction coefficient can be calculated in the same way (4):

$$\mu_e = \mu_s + \mu_a, \quad (4)$$

where  $\mu_s$  and  $\mu_a$  are the spatial densities of occurrence of extinction centers, respectively, the extinction coefficient is equal to the sum of the scattering and absorption coefficients.

In the matter of the behavior of light in tissues, the anisotropy coefficient is an important factor. This is the property of a material that allows it to change or take on different properties in different directions as opposed to isotropy. It can be defined as the difference, measured along different axes, in the physical or mechanical properties of a material (e.g., absorption).

The scattering anisotropy coefficient is defined as the mean value of the cosine of the scattering angle  $\theta$ . Denoting this coefficient by  $g$ , we can determine it from the relationship (5):

$$g = \langle \cos \theta \rangle = \int p(\theta) \cos \theta d\omega\Omega, \quad (5)$$

where:  $\langle \dots \rangle$  stands for the average value,  $p(s_2, s_1)$  is phase scattering function from angle  $s_1$  to angle  $s_2$  (6):

$$p(s_2, s_1) = \frac{\sigma_d(s_2, s_1)}{\sigma_d(s_1)} \quad (6)$$

The anisotropy factor can vary between -1 to 1 (where -1 means that all photons are scattered in the center of scattering in the direction opposite to the incident photon, and one means they are scattered in the direction of the incident photon). However, a value of  $g=1$  means no scattered photons. Despite having the same direction, a scattered photon may differ from the incident photon in other parameters, such as polarization, phase, or frequency for inelastic scattering.

All tissues have specific layered structures. Each layer also has its specific texture, which results in different compositions, different concentrations of light absorbers, and thus different optical parameters characterizing them. It is difficult to accurately distinguish the baseline absorption coefficient values associated with meaningless epidermis and bloodless dermis. So the baseline absorption of both epidermis and dermis is often approximated to a singular value for certain wavelength [9].

The interaction of light with multi-layered and multi-component skin, such as breast skin, is a very complex process. The light beam is transformed into scattered light by microscopic non-uniformities at the boundary between air and the stratum corneum layer of the epidermis. Most of the reflected light is caused by backscattering in various skin layers (stratum corneum, epidermis, dermis, and microvasculature). The analysis of light propagation in such structures is more complicated than inhomogeneous objects.

**Light source** Delivery systems for light can function as an isotropic point source that emits spherically symmetrical light fields, a line source that emits cylindrically symmetrical light fields, or a plane source that emits light fields with a one-dimensional variation.

The source of photons in the simulation is a point source generating photons in all directions, located inside the scattering medium at point P with coordinates  $x$ ,  $y$ , and  $z$ . Suppose we denote by  $s$  the unit vector describing the direction of the photon, in the case of a point source, for a given coordinate system Oxyz. In that case, it is sufficient to find two angles:  $\theta$  and  $\Psi$ , which respectively are the polar angle of propagation direction, i.e., the angle between the  $z$ -axis and  $s$ , and the angle between the  $x$ -axis and the projection of the vector  $s$  onto the Oxy plane.

A point light source is a theoretical light source that emits light rays from a single point. In practice, such a spot can be represented by a very small light source, an LED, or a thinner optical fiber tip that can emit light in one direction.

The characteristic of a point light source is the emission of light evenly in all directions, which means that the light rays propagate in all directions with the same intensity. However, real point light sources emit light slightly unevenly in different directions in practice due to technical limitations. Due to detector placement regarding a point source, a banana-like characteristic (Fig. 1b) is to be expected. We should note, that multiple photons paths may occur, and can differ from the illustrated case. The surface tissue has been distinguished as the photons can bounce off it. Please note that detector distance is calculated from the point light source to the closest edge of a detector.

**Photon movement simulation** In the case of the Monte Carlo method, these are calculations performed on millions of photons, making speed necessary. That's why it was decided to use C++ language for this issue. The Monte Carlo method involves random sampling of variables from well-defined probability distributions. The accuracy of the result obtained by this method depends on the number of checks but, above all, on the quality of the pseudo-random number generator used.

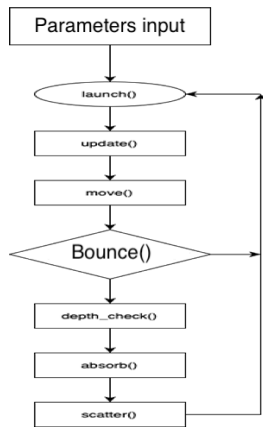


Fig. 2: Monte-Carlo simulation algorithm

Absorption, scattering, or reflection of a photon are physical phenomena that we want to simulate in the code. This program simulates light propagation from a normal irradiation medium with anisotropic scattering. It also records the escape of photons on the upper surface.

It was decided to use centimeters as the base unit of length throughout the simulation for consistency. The thickness of each layer and other distances from the user interface are given in mm. Absorption and scattering coefficients are given in  $\text{cm}^{-1}$ .

The program consists of individual blocks, as shown in Fig. 2. All of them are necessary to perform a correct simulation to analyze photon movement in tissues.

A simple variance reduction technique, implicit photon capture, is used to improve the performance of Monte Carlo simulations. This

technique allows multiple photons to propagate equivalently as a packet along a specific path simultaneously. Each photon packet is initially assigned a weight. The photon is injected perpendicularly into the tissue at the starting point, corresponding to a collimated, arbitrarily narrow beam of photons.

The current position of the photon is given by Cartesian coordinates  $(x, y, z)$  as shown in Fig. 1a. The photon's current direction is given by the unit vector  $r$ , which can be equivalently described in terms of direction cosines  $(\mu_{x_1}, \mu_{y_1}, \mu_{z_1})$ . The photon position is initialized to  $(0, 0, 0)$ , and the direction cosines are set

to  $(0, 0, 1)$ . When a photon is fired, if there is a mismatched boundary on the surface of the tissue, there could be some specular reflection.

The `move()` function changes the photon's position in the tissue. The position of the photon packet is changed by a quantitative substitution, which can be represented as (7):

$$x \leftarrow x + d \cdot \mu_x; y \leftarrow y + d \cdot \mu_y; z \leftarrow z + d \cdot \mu_z, \quad (7)$$

where  $d$  is the components of the guiding vector.

The guiding vector equals  $-\log(\text{rand-f}()+1,0)/(\mu_s + \mu_a)$  is a function that returns non-negative double-precision floating-point values evenly distributed in the range from 0 to 1. To generate a random number, the `rnm()` method is powered by a seed created based on the current system time so that the sequence of pseudo-random numbers differs each time the function is called. Then, a `uniform_real_distribution` class object is created with the name `unif`, which is initialized with the interval  $[0, 1]$ . This object is used to select a random number from a given range using the `unif(rng)` method.

Arrows indicate quantitative substitutions. Variables on the left have new values, and variables on the right have old values. The equals sign is used for this purpose in a real C program.

Once the photon takes a step, some mass attenuation of the photon due to absorption by the interaction site must be calculated. The local grid element will embed a fraction of the photon's current mass and weight.

After the photon packets have made their move and reduced their weight, the photon packet is ready for scattering. The probability distribution of the cosine of the deflection angle,  $\cos \theta$ , is described by the scattering function (8):

$$p(\cos \theta) = \frac{1 - g^2}{(1 + g^2 - 2g \cos \theta)^{3/2}}, \quad (8)$$

where the anisotropy,  $g$ , is defined as the average of the cosine of the scattering angle  $\theta$  and is between  $-1$  and  $1$ .

The cosine of  $\theta$  value is calculated using a function that returns pseudo-random numbers. With the anisotropy coefficient taking the value of 0, it is equal to the difference of double the pseudo-random number and one. For the rest of the value of the anisotropy coefficient, it is calculated based on the formula. To determine the new scattering direction, a new value of  $\mu_2$  is calculated using the coordinate values of the vector from the previous iteration. New direction values are computed in the `scatter()` function, and the following formulas are used (9) (10) (11):

$$\mu_{x2} = \frac{\sin \theta}{\sqrt{1 - \mu_{z1}^2}} (\mu_{x1} \mu_{x1} \cos \psi - \mu_{y1} \sin \psi) + \mu_{x1} \cos \theta \quad (9)$$

$$\mu_{y2} = \frac{\sin \theta}{\sqrt{1 - \mu_{z1}^2}} (\mu_{y1} \mu_{z1} \cos \psi + \mu_{x1} \sin \psi) + \mu_{y1} \cos \theta \quad (10)$$

$$\mu_{z2} = -\sin \theta \cos \psi \sqrt{1 - \mu_{z1}^2} + \mu_{z1} \cos \theta \quad (11)$$



where:  $\mu_{x_1}, \mu_{y_1}, \mu_{z_1}$  are the previous coordinates of the versor, and  $\mu_{x_2}, \mu_{y_2}, \mu_{z_2}$  calculated for later use in the next iteration.

If  $\mu_{z_1}$  is either 1 or -1 in the previous iteration, the direction values can be described as:

$$\mu_{x_2} = \sin \theta \cos \phi, \tag{12}$$

$$\mu_{y_2} = A \sin \theta \sin \phi, \tag{13}$$

$$\mu_{z_2} = A \cos \theta, \tag{14}$$

where:  $A = 1$  for  $\mu_{z_1} = 1$ , and  $A = -1$  for  $\mu_{z_1} = -1$ .

In the simulation of photon motion, the coefficients necessary to carry out the calculations, apart from absorption or scattering, are the anisotropy mentioned above or the number of photons to be sent into the tissue. The settings function reads these and other data, such as the depth of skin layers, from the data.csv file and writes them to the file array. The downloaded data is used to calculate the rest of the parameters used in the simulation. For a tissue model to serve well as a research tool, it must have properties close to those of real human tissue. The proposed tissue parameters used in our simulation are summarized in the Table. 1.

Table 1: Absorption and scattering coefficient depending on wavelength

Wavelength	940nm	850nm	760nm	565nm
$\mu_a$ [cm <sup>-1</sup> ] of skin	0,1634	0,227	0,326	0,854
$\mu_a$ [cm <sup>-1</sup> ] of fat	1,351	0,324	0,466	1,296
$\mu_a$ [cm <sup>-1</sup> ] of muscle	0,432	0,3	0,384	1,991
$\mu_s$ [cm <sup>-1</sup> ] of skin	6,938	8,071	9,546	14,892
$\mu_s$ [cm <sup>-1</sup> ] of fat	0,0126	0,0001	0,0001	0,0001
$\mu_s$ [cm <sup>-1</sup> ] of muscle	1,351	0,3244	0,466	1,295

In each step of the loop, a single line is read in the main function and processed by the split function, which breaks it into individual elements separated by commas and writes them to the file array. After the data is read from the file, they are assigned to the appropriate variables. Then, the values of the absorption and scattering coefficients are read, and on their basis, the albedo is calculated depending on the data loaded in a given iteration.

### 3 Implementation and simulation

#### 3.1 Sensor - Photodiodes and their parameters

Diode is an electronic component that allows current to flow in one direction. Photodiodes are semiconductor optoelectronic devices that change their electrical properties in response to light radiation. Photodiodes are used for detection, sensors, and control systems. The light emitted on the photodiode stimulates the

current flow in a specific direction. This flow is measured and used for light-level determination or object detection. Infrared LEDs are widely used in industry, medicine, science, and consumer equipment such as remote controls or IR camera illuminators. Light-emitting diodes work mainly in the near-infrared range from 700 to 1500 nm. The index of relative spectral sensitivity to wavelength indicates how sensitive the diode is to the light of different wavelengths. The RSS value is calculated as the ratio of either detector's or sensor's maximum output to the brightness of the light source at a specific wavelength. RSS is essential for visual detectors and sensors as it helps determine how well a particular detector or sensor is going to respond to visible light.

To illustrate the operation of various detectors, it was decided to perform simulations on numerous IR photodiodes. All four simulations are carried out for 1,000,000 photons, using the following parameters:

- The distance of the source from the detector - 0.6 cm,
- Anisotropy coefficient - 0.8, Refractive index - 1.5,
- The thickness of the first layer of skin - 3.5 mm,
- The thickness of the fat layer - 10 mm,
- The thickness of the muscle layer - 11.2 mm.

Absorption and scattering coefficients depending on the wavelength are given in Table 1.

**BPW21R photodiode** It is a round diode with a diameter of 5.9 mm [11]. For the simulation, we assume a diode with properties and dimensions (as a square, i.e., 2.8 x 2.8 mm, surface of 7.84 mm<sup>2</sup>) as the BPW21R diode. The wavelength that guarantees the highest sensitivity was used for the simulation. The simulation was performed for 565 nm. Traces of detected photons were plotted in Fig. 3a. Photons reached an average depth of 1.2 centimeters into the tissue. The intensity distribution of photon occurrences was presented as a heatmap in Fig. 3b.

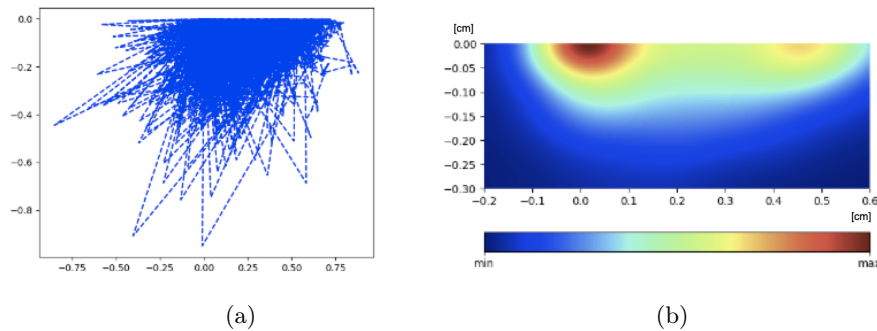


Fig. 3: BPW21R photodiode; (a) - MC simulation; (b) - MC simulation heatmap

**VBPW34S photodiode** The diode is rectangular and has a surface area of 7 mm<sup>2</sup> [12]. To simulate, the wavelength that provides the optimal sensitivity

was chosen - 940 nm. For the simulation, we assume a square with the same area but different dimensions of 2.65 x 2.65 mm. The photons detected by the detector reach up to 0.9 centimeters deep into the tissue, are shown in Fig. 4a, and clusters of light points are presented in Fig. 4b.

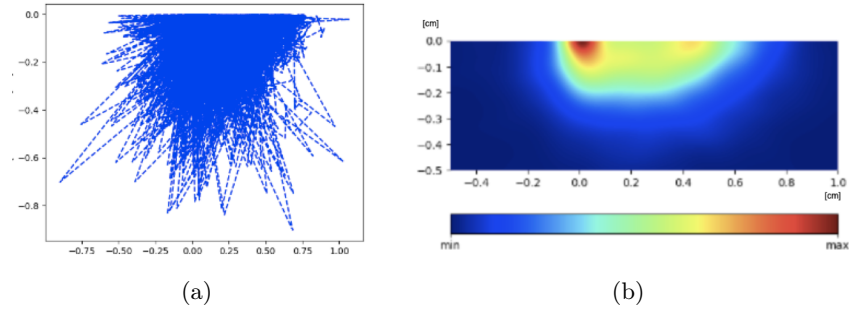


Fig. 4: VBPW34S photodiode; (a) - MC simulation; (b) - MC simulation heatmap

**SFH 203 photodiode** It is a through-hole diode with two contacts, dimensions 4.8 x 5.9 mm (surface 28.32 mm<sup>2</sup>) [13]. A wavelength of 850 nm was chosen to achieve the diode’s highest sensitivity. Photons detected that traveled more than a centimeter were shown in Fig. 5a. Photon concentration points are shown in Fig. 5b.

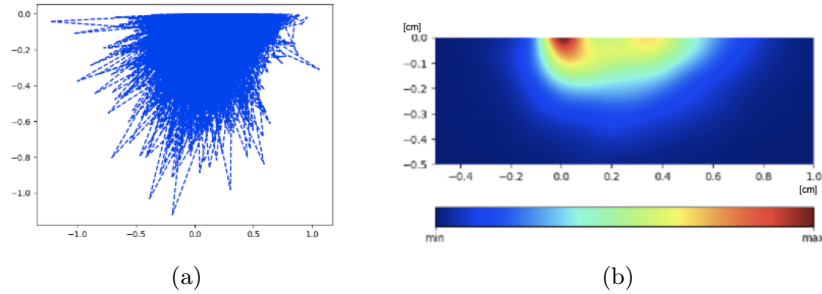


Fig. 5: SFH203 photodiode; (a) - MC simulation; (b) - MC simulation heatmap

**S10784 photodiode** It is a through-hole diode with two contacts, dimensions 4.1 x 4.7 mm (surface 19.27 mm<sup>2</sup>)[14]. To achieve the highest sensitivity of the diode, a wavelength of 760 nm was chosen. Photons detected by the detector reach about a centimeter deep into the tissue, shown in Fig. 6a. Clusters of light points can be seen in Fig. 6b.

For each photodiode, ten cycles of simulation were performed. A mean value and number of photons detected per 1 mm<sup>2</sup> (mean value of detected photons

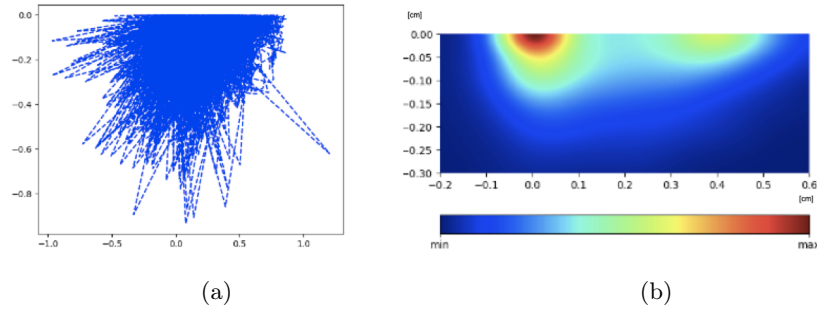


Fig. 6: S10784 photodiode: (a) - MC simulation; (b) - MC simulation heatmap

divided by photodiode active surface area) were later calculated. Results were presented in Table 2.

Table 2: Number of photons detected for different photodiodes during ten simulation cycles

Simulation No.	VBPW34S (940nm)	SFH 203 (850nm)	S10784 (760nm)	BPW21R (565nm)
1	762	2255	1077	295
2	784	2187	1053	307
3	794	2236	1083	298
4	786	2221	1066	302
5	776	2250	998	294
6	799	2195	1094	297
7	813	2228	1017	303
8	759	2294	1060	311
9	783	2213	1027	308
10	807	2230	1059	273
Mean	766.2	2230.9	1053.4	298.8
Mean photons value detected per 1 mm <sup>2</sup>	109.46	71.71	54.67	38.112

## 4 Results and Discussion

All four simulations performed on different types of IR photodiodes showed that the wavelength of the light affects the number of photons detected from the detector and the depth to which the radiation reaches. The lowest mean value of photons detected was observed for the BPW21R photodiode – an average of 298.8 (0.02988%) photons was detected. The SFH 203 photodiode was detected to be the highest value of photons averaging at around 2230.9 (0,22309%). As

the simulated wavelength decreased, so did the value of the mean photon detected per  $1 \text{ mm}^2$ . The lower absorption coefficient of skin and fat layers caused it. As this SFH203 has proved to be the most effective in detecting photons under predetermined conditions, it was decided to perform simulations for different variants of the detector. The distance of the source from the detector was changed. The dimensions of the photodiode are  $4.8 \times 5.9 \text{ mm}$ , and the wavelength of light used is  $850 \text{ nm}$ . In Fig.7a, the simulation results for different distances of the photon source from the detector were presented.

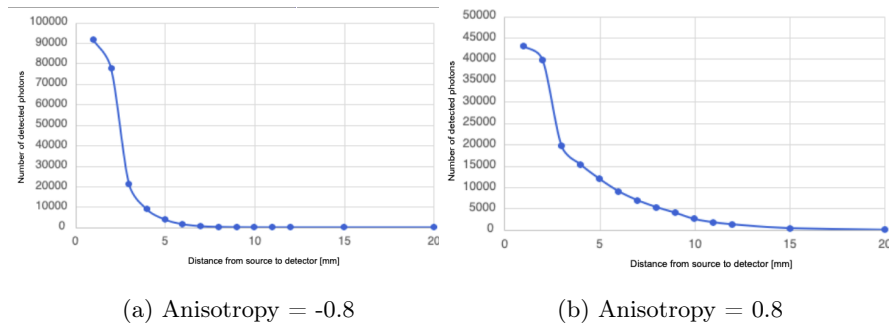


Fig.7: Number of detected photons depending on the transmitter - detector distance for different anisotropy coefficient

Also, simulations for an anisotropy coefficient equal to 0.8 (instead of -0.8) were performed. Results are shown in Fig. 7b. Even though for small anisotropy values number of detected photons was greater as the source-detector distance grew, the number of detected photons drastically decreased. Higher values of anisotropy allowed for simulations of many further regions of tissue. A low anisotropy coefficient is associated with a high degree of non-uniform distribution of photons in space. Due to this parameter and its low value, photons spread evenly to both sides of the source, not just one, as it would be in the case of a higher value of this parameter. During further experiments, the influence of the anisotropy factor on the detection ratio should be taken into account.

## 5 Conclusions

The aim of the work was to develop a tissue model and implement software for simulating the motion of photons using the Monte Carlo method. The simulation model takes into account factors such as the absorption, scattering, and reflection of photons by skin tissue, as well as the diffusion of photons through the skin. This allows researchers to study the effects of different wavelengths of light on blood flow and oxygenation in the skin.

We conclude that the Monte-Carlo simulation is a powerful tool for understanding the complex physics of photon interaction with skin tissue and can

help researchers develop new strategies for improving blood circulation and tissue oxygenation. Depending on the parameters selected by the user, the program reads the appropriate absorption and dispersion coefficients and simulates photon behavior in user-defined tissue. As a final result, information about the distribution of light intensity in the tissue and the number of photons absorbed in individual tissue locations is provided. This information can then be used to create visualize behavior of light in tissue or to study various optical properties of the tissues. A series of simulations for four models of photodiodes were performed. The following design guidelines were proposed:

- Since the ratio of detected to emitted photons is relatively small, a very sensitive measurement system should be designed. In sensor design, photodiodes with larger surface areas should be more effective.
- Photodiodes with their peak Relative Spectral Sensitivity within higher wavelengths exhibit higher photon detection ratio per 1 mm<sup>2</sup> ratio. Thus light sources and photodiodes working in NIR spectra should be considered
- Since the distance between the source and the detector highly affects the number of photons detected, it should be easily adjustable.

## References

1. IARC Homepage, <https://www.iarc.who.int/cancer-type/breast-cancer/>. Last accessed 21.03.2023
2. Mould R.: Cancer statistics overview with special reference to prostate, colon and rectum, lung, breast and cervix uteri, *Journal of Oncology* Vol 58, No 3, (2008)
3. Didkowska J., Wojciechowska U., Zatoński W.: Prediction of cancer incidence and mortality in Poland up to the year 2025, *Nationwide cancer database*, (2009)
4. Repež A., Oroszy D., Arnež ZM.: Continuous postoperative monitoring of cutaneous free flaps using near infrared spectroscopy. *Journal of Plastic, Reconstructive & Aesthetic Surgery* 61:71–77.
5. Rogoń I., Tojza P., Wittbrodt E., Łuszczek M., Jankau J.: Monte-Carlo modeling of optical sensor for post-operative free flap monitoring, *Information technology in biomedical engineering*, pp. 141-153, (2021)
6. Hossain, S., Kim, K.-D.: Non-Invasive In Vivo Estimation of HbA1c Using Monte Carlo Photon Propagation Simulation: Application of Tissue-Segmented 3D MRI Stacks of the Fingertip and Wrist for Wearable Systems. *Sensors* 2023, 23, 540.
7. Carlson M., Alt-Holland A., Egles C. And Garlick J., *Three-Dimensional Tissue Models of Normal and Diseased Skin* 1,2,3, (2008)
8. Micheels J., Alsbjorn B., Sorensen B.: Laser doppler flowmetry. A new non-invasive measurement of microcirculation in intensive care? *Resuscitation*. (1984)
9. Jacques S.: *Skin Optics*, Oregon Medical Laser Center News. (1998)
10. Metropolis N., *THE BEGINNING of the MONTE CARLO METHOD*, Los Alamos Science Issue 1987
11. Vishay, Silicon Photodiode BPW21R, 81519 datasheet, Rev. 1.7, (2011)
12. Vishay, Silicon PIN Photodiode VBPW34S, VBPW34SR, 81128 datasheet, (2011)
13. Osram, SFH203 Radial T1 3/4 Silicon PIN Photodiode, Rev. 1.3, (2018)
14. Hamamatsu, Si PIN photodiodes S10783, S10784, KPIN1079E02 datasheet, (2012)
15. Plucinski, J.: *Optyka nieuporządkowanych ośrodków silnie rozpraszających (Optics of highly scattering random media)*, Monografie 102, Wydawnictwo Politechniki Gdańskiej, ISBN:978-83-7348-300-9, Gdańsk, Poland, (2010)

